Electrochimica Acta 298 (2019) 484–495

Contents lists available at ScienceDirect

Electrochimica Acta

journal homepage: www.elsevier.com/locate/electacta

Physiological monitoring of tissue pH: *In vitro* characterisation and *in vivo* validation of a quinone-modified carbon paste electrode

Karen M. Herdman, Carmel B. Breslin, Niall J. Finnerty*

Chemistry Department, Maynooth University, Co. Kildare, Ireland

ARTICLE INFO

Article history:
Received 9 October 2018
Received in revised form
18 December 2018
Accepted 21 December 2018
Available online 21 December 2018

Keywords:
In vivo
Ischaemia
pH
Continuous monitoring
Voltammetry

ABSTRACT

The fluctuation of physiological pH from homeostatic levels has the potential to cause life threatening complications unless counteracted in a timely manner. Therefore, the development of reliable and accurate sensors for the continuous monitoring of pH is of vital importance for clinical monitoring. Herein, we describe the extensive *in vitro* characterisation of a quinone-modified carbon paste electrode (CPE) and its subsequent *in vivo* validation in the peripheral tissue of anaesthetised rats. Sensocompatibility investigations identified stable and accurate measurements in lipid (phosphatidylethanolamine; PEA) and protein (bovine serum albumin; BSA) solutions when the pH sensor was continuously cycled for nine hours in the physiological contaminants. The influence of endogenous electroactive molecules e.g., ascorbic acid and uric acid and pharmacological interferents e.g., acetaminophen and acetylsalicylic acid was deemed negligible on the pH sensitive peak. Furthermore, there was no impact of ionic strength and the quinone oxidation peak remained selective for H^+ over other endogenous cations. The effect of temperature and a pseudo reference electrode (PRE) on the sensor performance have also been elucidated. The efficacy of the modified-CPE to respond to *in vivo* tissue pH dynamics was demonstrated using a model of peripheral ischaemia and sodium bicarbonate injections. Collectively, this body of evidence clearly support the ability of the quinone-modified CPE to continuously measure pH fluctuations under physiological conditions.

1. Introduction

Real-time monitoring of physiological pH levels is important for many reasons. For example, abnormal tissue pH is an indicator of altered cellular metabolism in diseases including stroke [1] and cancer [2]. In particular, tissue ischaemic injury, i.e. reduced blood flow, is one of the most common types of injury in clinical medicine [3–5]. Ischaemic tissue is generally caused by obstruction of an artery. The affected tissue often becomes acidic due to increased anaerobic respiration leading to irreversible cellular damage. The first investigations into the relationship between pH levels and ischaemia were reported nearly 35–40 years ago, identifying that tissue pH falls during an ischaemic event [6–8]. Researchers agreed that tissue pH fell as the decrease in blood flow to the tissue resulted in anaerobic metabolism, which consequently produced lactate. The presence of lactate contributes to an increase in H^+ ion activity, which is proportional to a decrease in pH. Thus, pH can be used as an indication of a reduction of tissue perfusion [6,7,9].

In-vivo sensors can provide an instant evaluation of a biological parameter such as tissue pH [10]. For this purpose, small devices with low drift, easy calibration, immunity to electrode fouling and long life-time are required. Wolpert et al. compared serum pH measurements to that of tissue pH [7]. They found that tissue pH, when compared to serum pH, had the advantages of reacting earlier to changes in tissue perfusion and it could be measured with minimal invasiveness. These studies involved miniaturised glass pH sensors, whose major disadvantages lie in the difficulty of miniaturisation [11], drift [12], fragility [13] and electrode fouling [14], culminating in inaccurate measurements. Voltammetric pH sensors have recently demonstrated excellent potential both *in vitro* [15–17] and *in vivo* [18,19]. They function by measuring the redox potential of a pH dependent moiety, as described by the Nernst equation.

$$\mathbf{E} = \mathbf{E}^0 + (\boldsymbol{RT}/\boldsymbol{F}) \ln [\mathbf{a_H}^+] \quad (1)$$

* Corresponding author.
E-mail address: niall.finnerty@mu.ie (N.J. Finnerty).

https://doi.org/10.1016/j.electacta.2018.12.110
0013-4686/

$$\mathbf{E = E^0 - (2.303RT/F)\,pH} \quad (2)$$

where E is the measured potential, E^0 is the standard electrode potential, *R* is the universal gas constant, T is the temperature in Kelvin and *F* is the Faraday constant.

When characterising a voltammetric pH sensor capable of continuous *in-vivo* measurements, certain criteria should be maintained. The sensor should be easily miniaturised in order to inflict minimal trauma to the insertion site, thereby reducing the risk of infection to the subject. Also, the pH response should remain stable, with minimal drift, over a constant recording period. In addition, it should demonstrate a fast response time and be independent of temperature, cation and ionic strength fluctuations. Minor changes in pH can be detrimental *in vivo*, meaning the sensitivity should be linear over a physiologically relevant range. In healthy patients, the pH of the blood varies between 7.35 and 7.45; anything outside 6.8 and 7.8 may result in irreversible cell damage and eventual death [20–23]. The voltammetric response of an *in vivo* sensor should not be compromised by the presence of electrochemically active moieties found ubiquitously throughout tissue. It is pivotal to device functionality that selectivity towards the target species is retained in such a scenario. Physiologically relevant metal ions can be detrimental to the voltammetric signal, e.g., Ca^{2+} and Mg^{2+} and their impact on sensor performance must be elucidated.

Biofouling of implanted electrochemical sensors occurs immediately upon contact with living tissue, through physiological responses from endogenous protein and lipid adsorption. This can limit the mass transport rate at the electrode surface [24], thereby affecting the voltammetric signal produced by functionalised CPEs. The lipophilic nature of biological tissue has been reported to remove the hydrophobic oil from the CPE [25], thus altering and potentially compromising the modified surface. Such considerations are one of the major hurdles that need addressing during the characterisation of an *in vivo* sensor. In addition to protein and lipid fouling, the physiological environment is populated with a myriad of endogenous electroactive interferents. It is therefore pivotal for the successful characterisation of a voltammetric pH sensor *in vivo* that peak resolution is maintained in the presence of such interferents. Furthermore, changes in ionic strength give rise to changes in the conductivity of a solution. For example, decreasing the ionic strength of a solution decreases the conductivity, hence increasing the solution resistance. This results in an increased IR drop causing a subsequent potential increase which modifies the observed potential and may impact on voltammetric potential.

Herein, we describe the *in vitro* characterisation of a recently reported pH sensitive carbon paste electrode (CPE) [26]. The electrodeposition of the diazonium salt, 4-Benzoylamino-2, 5-dimethoxybenzenediazonium chloride - hemi zinc chloride (FBRR), onto CPEs was optimised, to produce a pH sensor that has demonstrated excellent stability and Nernstian behaviour over the physiological range 7.2–7.6. Furthermore, increasing the number of calibration points from three to *ca.* 40 had no significant impact on the sensor's sensitivity and shelf-life investigations identified retention of the FBBR-modified CPE sensitivity over 28 days when stored under air conditions at 4 °C [26]. CPEs have demonstrated excellent long term stability for *in vivo* monitoring of brain tissue [24,27], an environment they are particularly suited to since the interaction between the pasting liquid and brain lipids reduces the electrode fouling caused by the proteins [24]. However, the effect on functionalised CPEs is not well known and the impact on the covalently bonded pH moiety was investigated within. The effect of interferents, cations, ionic strength, temperature and a pseudo reference electrode (PRE) is also discussed in detail. Finally, the characterised sensor was implanted into the hind limb of anaesthetised rats and continuous monitoring of tissue pH was performed. Perturbations of tissue pH were undertaken through a previously described hind limb ischaemia model [28] and local injections of sodium bicarbonate. During ischaemia, a reduction in oxygen levels should lead to a concurrent decrease in tissue pH [29] arising from increasing lactic acid concentrations caused by the switch to anaerobic metabolism. Conversely, injections of sodium bicarbonate [30–32], a weak base, were administered locally to the hind limb of the animals to induce an increase in tissue pH. Increasing the bicarbonate concentration in the tissue will cause the acid-base equilibrium to shift to more alkaline, resulting in an increase in pH.

$$\mathbf{HCO_3^- + H^+ \leftrightarrow CO_2 + H_2O} \quad (3)$$

Furthermore, post *in vivo* calibrations performed on the FBRR-modified CPE determined no significant difference from pre-implantation sensitivities. Collectively, the body of work described within demonstrates the efficacy of the FBRR-modified CPE at measuring reliable and accurate changes in physiological pH.

2. Materials and methods

2.1. Chemicals and solutions

All reagents used i.e., sodium chloride (NaCl), sodium hydroxide (NaOH), sodium hydrogen phosphate (NaH_2PO_4), 4-benzoylamino-2, 5-dimethoxybenzenediazonium chloride - hemi zinc chloride (FBRR), graphite powder (<20 μm, 1.9 g/cm^3), ilicon oil (0.96 g/mL), bovine serum albumin (BSA), phosphatidylethanolamine (PEA), ascorbic acid, L-cysteine, L-gluthathione, L-tyrosine, uric acid, acetaminophen, acetylsalicylic acid, dopamine hydrochloride, 3, 4-dihydroxyphenylacetic acid (DOPAC), 5-hydroxy-indole acetic acid (5-HIAA), calcium chloride, magnesium chloride were purchased from Sigma Aldrich Chemical Co. (Dublin, Ireland). Sulfuric acid was purchased from VWR International Ltd (Dublin, Ireland). Calibrations were performed in phosphate buffered saline (PBS); NaCl (0.15 M), NaOH (0.04 M) and NaH_2PO_4 (0.04 M) made up in doubly distilled deionised water. The pH was adjusted accordingly using a laboratory pH meter (Eutech Instruments, Ayer Rajah, Singapore).

2.2. Electrode manufacture and preparation

CPEs were manufactured from Teflon®-insulated silver (Ag) wire (200 μm bare diameter 8T, Advent Research Materials; Oxford, UK) as described previously [26]. A 5 cm length of Teflon insulated Ag wire was cut. Approximately 1 mm of the Teflon® insulation was removed from one end, exposing the bare Ag wire. Using a tweezers, the Teflon® was gently moved along the length of the wire, exposing a 1 mm cavity at the opposite end of the electrode. The cavity was packed with carbon paste (0.71 g graphite powder (<20 μm, 1.9 g/cm^3) and 250 μL silicon oil (0.96 g/mL)). The exposed Ag wire at the opposite end was soldered into a gold clip (Fine Science Tools GmbH, Heidelberg, Germany). A bare Ag wire with the same diameter, was used as a plunger, to ensure that the paste was compactly packed. The surface was then levelled by gently rubbing it on a clean, flat surface. The electrochemical deposition of the quinone containing aryl diazonium salt, FBRR, onto CPEs was achieved by a one-step electrochemical reduction process in 0.1 M H_2SO_4 using Linear Sweep Voltammetry (LSV) [26]. The first step of the proposed mechanism involves the electrochemical reduction of the aryl diazonium cation (Ar-N_2^+) to form the corresponding aryl radical (Ar·), with the loss of N_2, as described in Equation (4). The second step occurs when the radical reacts with

the CPE surface, and a strong covalent C–C bond is formed according to Equation (5):

$$\mathbf{ArN_2^+ + 1\,e^- \rightarrow Ar^{\cdot} + N_2} \quad (4)$$

$$\mathbf{Surface + Ar^{\cdot} \rightarrow Surface - Ar} \quad (5)$$

2.3. In vitro investigations

All FBRR-modified CPEs were cycled in N_2 (BOC Ireland) saturated PBS over the potential ranges −0.7 V to +0.8 V, *vs.* SCE at 100 mV/s. According to Scheme 1, the redox activity of the deposited diazonium salt involves a $2e^-$ oxidation, converting the methoxy to the equivalent quinone, followed by a $2e^-/2H^+$ exchange to form the hydroxy-quinone. The potential at which the redox reactions take place are pH dependent resulting from the protonation/deprotonation of the quinone [26].

For calibrations performed during Sections 3.3 to 3.7; once cycling at one pH was complete (50 cycles), the electrodes were removed from one PBS solution, rinsed in deionised water and placed in another. The cycling order in the respective pH solutions was randomised between electrodes. A saturated calomel electrode (SCE) was used as the reference electrode, unless stated otherwise, and a large Pt wire served as the auxiliary electrode. Sensocompatability investigations were performed on separate sets of FBRR-modified CPEs ($n = 4$) that were either stored for 24 h or continuously cycled for 400 and 1100 cycles, in 1% solutions of BSA and PEA over the potential range −0.7 V to +0.8 V. The effect on the quinone peak resolution and stability was investigated and compared for both conditions.

Interference investigations were performed by cycling FBRR-modified CPEs in PBS containing a physiologically relevant concentration of the respective interferents; ascorbic acid (500 μM), L-cysteine (100 μM), L-glutathione (100 μM), L-Tyrosine (200 μM), uric acid (100 μM), acetaminophen (500 μM) and acetylsalicylic acid (500 μM). The effect of the interferent on the quinone peak resolution was elucidated.

$$\mathbf{I = 0.5 \sum z^2_i c_i} \quad (6)$$

The ionic strength of the solutions was calculated using Equation (6), where z is the charge and c represents the concentration of the ions. Using this Equation, the ionic strength of the PBS was altered to give ionic strengths of 0.46 M, 0.92 M and 0.23 M and the sensitivities compared. Selectivity investigations were performed by cycling FBRR-modified CPEs over various pH, in the presence of excess concentrations of Ca^{2+} (1.6 mM) and Mg^{2+} (21 mM). The sensitivities were compared against those obtained in standard PBS solution without the cations present.

Temperature investigations involved increasing the temperature of the PBS solution to 37 °C using a digital water bath and the sensitivity was determined and compared against that obtained at 25 °C. Finally, the effect of incorporating a PRE into the design was elucidated. Ag/AgCl-PREs were constructed from Teflon®-insulated Ag wire using a previously described protocol [33]. A 5 mm cylinder was prepared by removing the Teflon® from one end of the electrode. The 5 mm Ag cylinder (anode) and a corresponding Pt or Ag wire (cathode) were immersed in 1.0 M HCl for 30 s which resulted in the formation of a Ag/AgCl layer. The sensitivities were compared against those obtained using a conventional SCE.

2.4. In vivo surgical protocol

Male Wistar rats (Charles River, UK, 400–600 g) were housed with a maximum of three per cage in a temperature (17–23 °C), humidity, and light controlled (12 h light, 12 h dark cycle) environment at Maynooth University. Food and water were available *ad libitum*. The subjects were allowed to acclimatise for at least one week prior to surgery. The rats were anesthetised with Isoflurane anaesthesia (Abbott Laboratories, Dublin, Ireland) in the supine position with the anaesthesia mask fixed tightly around the nose. The subject was kept on a heating pad for the duration of the recording to prevent hypothermia. An 18-gauge needle (inner diameter = 0.84 mm) which contained the FBRR-modified CPE,

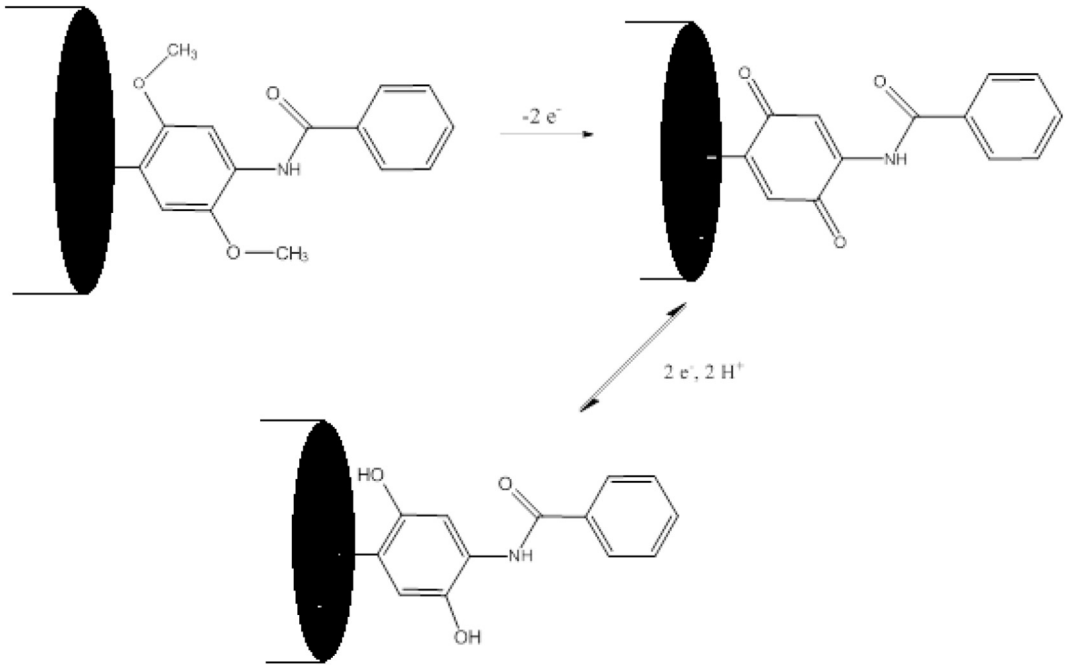

Scheme 1. Redox activity of electrodeposited quinone group on FBRR-modified CPE.

auxiliary electrode and Ag/AgCl-PRE, was inserted into the hind-limb to a depth of *ca.* 1 cm (see Fig. 1). Once implanted, the hypodermic needle was retracted from the tissue leaving the electrodes in place. All recordings were carried out with the subjects under general anaesthesia. Subjects were euthanised upon completion of recordings by intraperitoneal injection of Euthatal. All experimental procedures were approved by Maynooth University Ethics Committee and performed under license in accordance with the European Communities Regulations 2002 (Irish Statutory Instrument 165/2013).

2.5. In vivo voltammetric investigations

All electrodes were connected via gold electrical contacts to the data acquisition equipment. Cycling of the FBRR-modified CPE, over the potential range −0.7 V to +0.8 V *vs.* Ag/AgCl at 100 mV/s, was carried out over a 45-min period (90 cycles) to establish a baseline peak potential prior to the perturbation. The mean quinone peak potential was plotted against time for the analysis provided in Fig. 7. During ischaemia investigations (represented by shaded area in Fig. 7A), a tourniquet was placed around the subject's limb in close proximity to the body to facilitate occlusion of the blood supply as described previously [28]. Ischaemia was induced by pulling the tourniquet as tight as possible, verified visually by the increasing pallor of the subject's foot, and was maintained for a 10-min period. Once completed, the tourniquet was removed and recordings continued for a further 45 min (90 cycles). Similarly, during sodium bicarbonate investigations, cycling of the FBRR-modified CPE was carried out over a 45-min period (90 cycles) to facilitate baseline recordings. Subsequently, 100 μL volumes of 45 mM sodium bicarbonate were injected directly into the tissue containing the electrodes after 55, 60 and 65 min (represented by shaded areas in Fig. 7B). Cycling continued for a further 45 min (90 cycles). In total, each recording was performed for 100 min. Upon completion of the recordings, the FBRR-modified CPEs were removed from the hind limb and rinsed with deionised water. They were then recalibrated as described in Section 2.3 and the sensitivities compared against the pre-implantation values.

2.6. Instrumentation, software and data analysis

Voltammetric experiments were performed *in vitro* using a low-noise potentiostat (ACM Instruments, Cumbria, UK) and converted using an A/D converter (PowerLab, ADInstruments, Oxford, UK). *In vivo* recordings were performed using a Quadstat (eDAQ Ltd., Sydney, Australia) and converted using an A/D converter (eCorder, eDAQ Ltd.). The CV signals were recorded using eChem software (v2.1.16, eDAQ Ltd., Sydney, Australia) running on a Dell laptop. All *in vitro* pH sensitivities were calculated using linear regressions. For *in vivo* analyses, the mean quinone peak potential was plotted against time for the analysis provided in Fig. 7. The number of electrodes used is denoted by *n* except for *in vivo* investigations whereby *n* denotes the number of animals. Significant differences were calculated using the Student's *t*-test and one-way ANOVAs followed by Bonferroni *post hoc* test were performed where appropriate. The standard 95% confidence interval was used for these tests, so a *p*-value less than 0.05 indicated a significant difference between the data sets, whereas a *p*-value higher than 0.05 indicated no significant difference. These analyses were performed using GraphPad Prism® version 5.01 (GraphPad Software Inc., San Diego, CA, USA). Scanning Electron Microscopy (SEM) analysis was carried out using a Hitachi S-3200-N, with a tungsten filament electron gun that has a maximum magnification of 200,000x and resolution of 3.5 nm. A 5 mm long section was cut from the active end of the CPE. The Teflon® was carefully removed from the bottom 2 mm, and the exposed silver wire was angled to 90° and placed onto 12 mm carbon adhesive tabs (Agar Scientific), mounted on 15 mm × 6 mm specimen stubs (Agar Scientific), so that the modified surface was *ca.* 90° to the mount. The stubs were placed in the sputter coater and a vacuum was applied for 30 min. Sputter coating was performed, under argon, with an Au/Pd target, until a thickness of 5 nm was obtained.

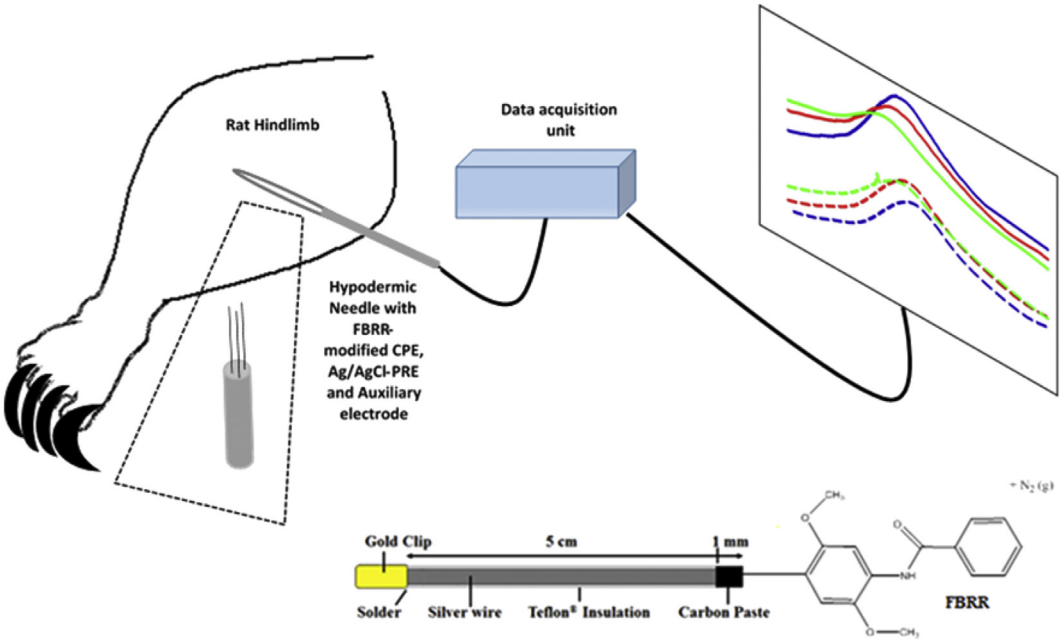

Fig. 1. Graphic illustration of *in vivo* recording set-up in the hind limb of anaesthetised rats and electrodeposited 4-benzoylamino-2, 5-dimethoxybenzenediazonium chloride - hemi zinc chloride (FBRR) on carbon paste electrode (CPE).

3. Results and discussion

3.1. Sensocompatability investigations

FBRR-modified CPEs were exposed to aqueous solutions of the protein, BSA and the lipid, PEA, to determine the effect on the anodic peak stability and resolution. Both have been utilised previously to characterise the response of electrochemical sensors to *in vivo* conditions [25,34–37]. The material-tissue interaction that results from sensor implantation is one of the major obstacles in developing viable, long term implantable sensors. The effect of storing FBRR modified CPEs for 24-h in 1% BSA solution is detailed in Supplementary Fig. SM1A. It is apparent that the anodic peaks are retained, however, the peak resolution has been greatly compromised and the peak potential shifted slightly. This can be attributed to the adsorption of protein molecules onto the electrode surface. The tendency is to build up a layer, inhibiting electron-transfer processes and resulting in an altered voltammogram [38]. This finding was not entirely unexpected. To determine the impact of applying a constant potential profile to the electrode surface in the BSA solution, the FBRR-modified CPEs were continuously cycled in the 1% BSA solution for 3.5 h (see Fig. 2A) and 9 h (see Fig. 2B). There is a huge improvement in the peak resolution in contrast to FBRR-modified CPEs stored in 1% BSA for 3.5 h (see Fig. SM1B). It is apparent that the constant application of an oxidation potential followed by a reduction potential prevents the protein layer from building up on the surface. A plausible explanation for this is detailed in Fig. SM1C. Increasing peak currents were observed during continuous cycling of the modified CPE in PBS which can be attributed to the gradual loss of silicon oil from the carbon paste. This loss of oil could prevent the build-up of large deposits of BSA on the surface. Furthermore, trace amounts of BSA remaining on the electrode surface may in fact enhance electron transfer [39] resulting in improved peak resolution and definition. In contrast the broader peaks with reduced definition present in Fig. SM1A and B are indicative of a decrease in electron transfer. The continuous cycling would be more representative of the targeted application in peripheral muscle monitoring supporting the stability of the pH sensitive moiety on the CPE surface.

The effect of storing the CPEs in 1% PEA for 24 h is illustrated in Fig. SM1D. As described earlier, a broad, ill-defined anodic peak was recorded post-storage which was to be expected, due to the well-established ability of lipids to remove the hydrophobic elements from the electrode surface, producing a more carbon powder like morphology [25]. Notwithstanding this, the effect of continuous cycling in PEA solution identified an improvement in peak intensity and resolution over 3.5 h (see Figure 2C) and 9 h (see Fig. 2D), albeit with slight shifts observed in the latter over the course of the cycling. These findings suggest that the PEA had not fouled the surface. Moreover, it suggests that it had enhanced the electron

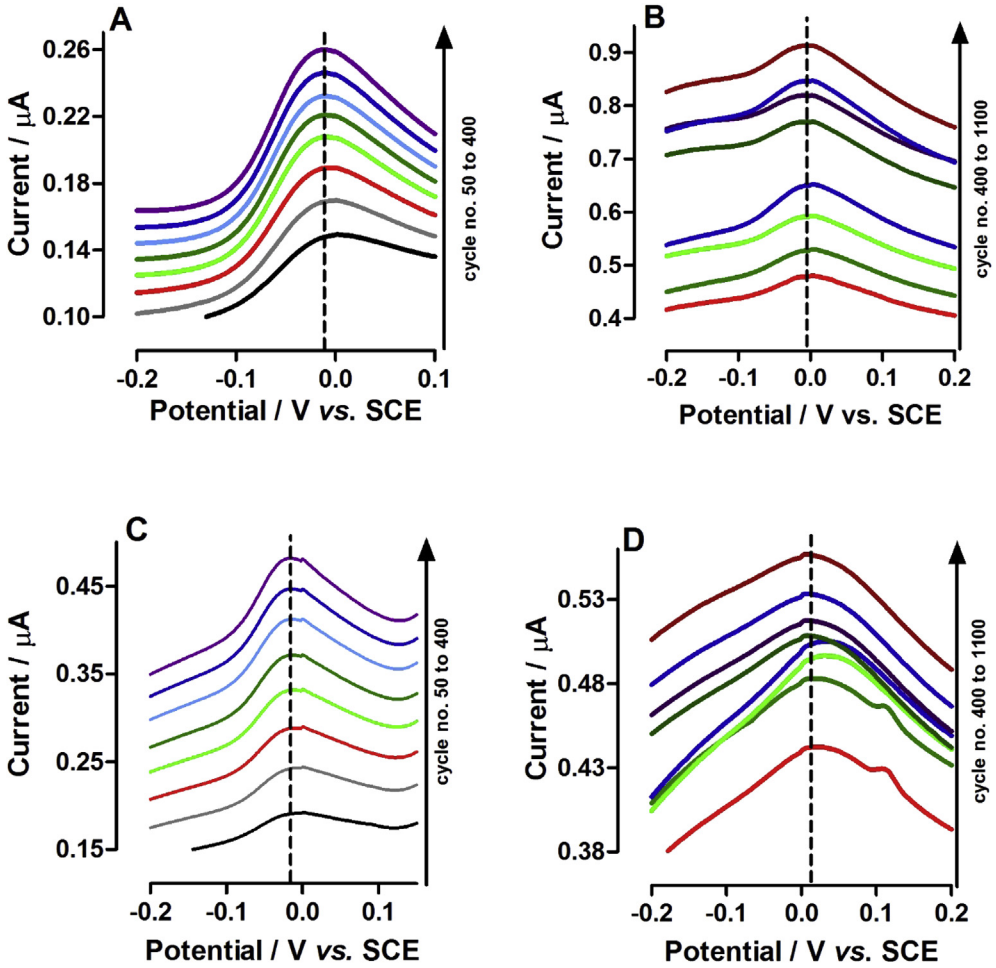

Fig. 2. Effect of continuous cycling on FBRR-modified carbon paste electrodes (CPE) anodic peak potentials in 1% bovine serum albumin (BSA) for (A) 400 cycles, (B) 1100 cycles and in 1% phosphatidylethanolamine (PEA) for (C) 400 cycles, (D) 1100 cycles. FBRR-modified CPEs cycled over potential range − 0.7 V to +0.8 V *vs.* saturated calomel electrode (SCE) at 100 mV/s ($n = 4$). Voltammograms performed at each 50th cycle included in A/C and each 100th cycle in B/D.

transfer kinetics. Conversely, the peak current was reduced when the electrodes were stored in lipid for 3.5 h as highlighted in Fig. SM1E. The application of the constant potential profile facilitated the adsorption and desorption of trace amounts of PEA on the CPE surface, preventing the build-up of the lipid layer. Collectively, these findings support the ability of the FBRR-modified CPE to perform stable measurements under physiological conditions, for a minimum of 9 h, through application of a constant potential profile.

3.2. Interference investigations

The FBRR-modified CPEs were cycled in PBS containing physiologically relevant concentrations of interferents present in peripheral interstitial fluid. The principal objective of this interference study was to confirm retention of the pH sensitive quinone peak in the presence of endogenous interferents. Table 1 details the findings from these investigations and Fig. 3 and SM2 illustrate the voltammograms recorded for each. There was a potential change recorded in the presence of certain interferents which was attributed to a shift in the pH of the solution. Examples of this are illustrated in Fig. 3. The voltammetric profile was repeated with the pH adjusted back to 7.4 and statistical analysis performed on the potential difference recorded for the quinone peak in the presence and absence of the interferent. In summary, there was no significant difference ($p > 0.05$) observed in quinone peak potential, in the presence of a physiological concentration of the endogenous species; ascorbic acid, uric acid, L-cysteine, L-tyrosine or L-gluthathione. Furthermore, two of the most commonly prescribed medications in clinical practice; acetaminophen and acetylsalicylic acid, had no significant effect ($p > 0.05$) on the pH sensitive peak potential, at clinically relevant concentrations. Moreover, the change in pH observed in the presence of the interferents validated the ability of the quinone peak to shift potential in the presence of the interferent. In addition, voltammetric data obtained over an extended calibration range (pH 6.0–8.0, see Fig. 4A) supports our assumption further. The largest anodic potential recorded was $< +100$ mV at pH 6.0. It is obvious from Fig. 3 and SM2 that there will be no contribution from any interfering agent at this potential, supporting retention of the quinone peak at this pH value. This can be best described by Fig. SM3A and B whereby clear and resolved redox peaks attributed to uric acid and acetaminophen, respectively, are clearly visible. However, there is no impact on the quinone oxidation peak due to the larger anodic potentials recorded for the interferents. In addition, the sensitivity of the FBRR-modified CPE, calculated for the pH range 6.0–8.0, was -58 ± 2 mV/pH ($n = 5$, $r^2 > 0.99$). This value is not significantly different ($p = 0.90$) than the sensitivity calculated over the pH range 7.2–7.6 (-59 ± 3 mV/pH, $n = 37$, $r^2 > 0.99$) which we reported previously [26]. This finding reinforces the ability of the FBRR-modified CPE to function over a larger pH range, however, to focus more closely on basal pH recordings, all further characterisation data was performed over the shorter pH range of 7.2–7.6.

Despite peripheral monitoring being the core application of this design, Table SM1 and Fig. SM3 highlight the selectivity characteristics of the FBBR-modified CPE against known interferents in the brain extracellular fluid for a broader range of applications. There was no significant difference ($p > 0.05$) recorded in the anodic peak potential when cycled in the presence of dopamine, DOPAC and 5-Hydroxy-Indole Acetic Acid.

3.3. Ionic strength investigations

The effect of ionic strength on the FBRR functionalised electrodes was tested by cycling the modified electrodes in PBS of altered ionic strength over the chosen pH range. Many pH sensors, in particular those pertaining to optical measurements, have a basic disadvantage of measuring signals that depend on the ionic strength of the sample [40]. It is obvious from Fig. 4B that excellent linearity was observed across all ionic strengths ($r^2 > 0.99$). There was no significant difference ($p = 0.18$, one-way ANOVA) observed across the sensitivities recorded in 0.23 M (-60 ± 1 mV/pH, $n = 4$), 0.46 M (-54 ± 3 mV/pH, $n = 4$) or 0.92 M (-58 ± 1 mV/pH, $n = 3$). Furthermore, Bonferroni *post hoc* analysis identified no significant variation between the respective ionic strengths. These findings confirm that increasing and decreasing the solution conductivity failed to cause a significant variation in the sensor performance across the varying pH range.

3.4. Cation selectivity investigations

It was imperative to investigate the selectivity of the quinone anodic peak for H^+ ions in solution. This was confirmed by introducing increased concentrations of Mg^{2+} and Ca^{2+} which are two of the most prevalent cations found in biological systems with average concentrations of 5 mM [41,42] and 1.2 mM [43], respectively. They are also known to form coordinate bonds and complexes with several quinones [44,45] and could therefore affect their redox peak potentials. Fig. 5A and B detail the effect of increasing Mg^{2+} and Ca^{2+} concentrations respectively, with excellent linear responses observed across all concentrations. Initial calibration of the FBRR-modified CPEs resulted in a sensitivity value of (-54 ± 2 mV/pH, $n = 4$). No significant difference was recorded in increased [Mg^{2+}] (-55 ± 4 mV/pH, $n = 4$, $p = 0.78$) and [Ca^{2+}] (-56 ± 2 mV/pH, $n = 4$, $p = 0.49$) in PBS, confirming the selectivity of the quinone anodic peak for H^+ over these cations. This excellent selectivity for H^+ ions is in close agreement with work described previously by Makos et al. using FBRR on carbon fibre electrodes [2]. This suggests a higher affinity of the quinone group for protons over the respective cations in solution. This is to be expected since quinone groups are well-established as being pH dependent and have been developed for the determination of pH [15,16,46].

Table 1
Effect of physiological interferents (Int) on FBRR-modified CPEs anodic peak potentials ($n = 4$). Data presented as ΔEp whereby ΔEp = Ep (Int) − Ep (PBS) and $\Delta Ep_{adjusted}$ = Ep (Int, pH adjusted) − Ep (PBS). *p*-value calculated from Ep (Int, pH adjusted) *vs.* Ep (PBS).

Interferent (Int)	ΔEp, mV Ep (Int) − Ep (PBS)	$\Delta Ep_{adjusted}$, mV Ep (Int, pH adjusted) - Ep (PBS)	p-value
Ascorbic acid	−4 ± 6 pH 7.31	1 ± 6 pH 7.40	0.86
Uric acid	n/a	0 ± 4 pH 7.40	0.92
L-Cysteine	−9 ± 3 pH 7.34	−5 ± 3 pH 7.40	0.10
L-Tyrosine	−2 ± 2 pH 7.38	−1± 2 pH 7.40	0.73
L-Glutathione	−3 ± 2 pH 7.36	−1 ± 2 pH 7.40	0.96
Acetaminophen	−6 ± 2 pH 7.34	−2 ± 2 pH 7.40	0.31
Acetylsalicylic acid	1 ± 3 pH 7.34	1 ± 2 pH 7.40	0.52

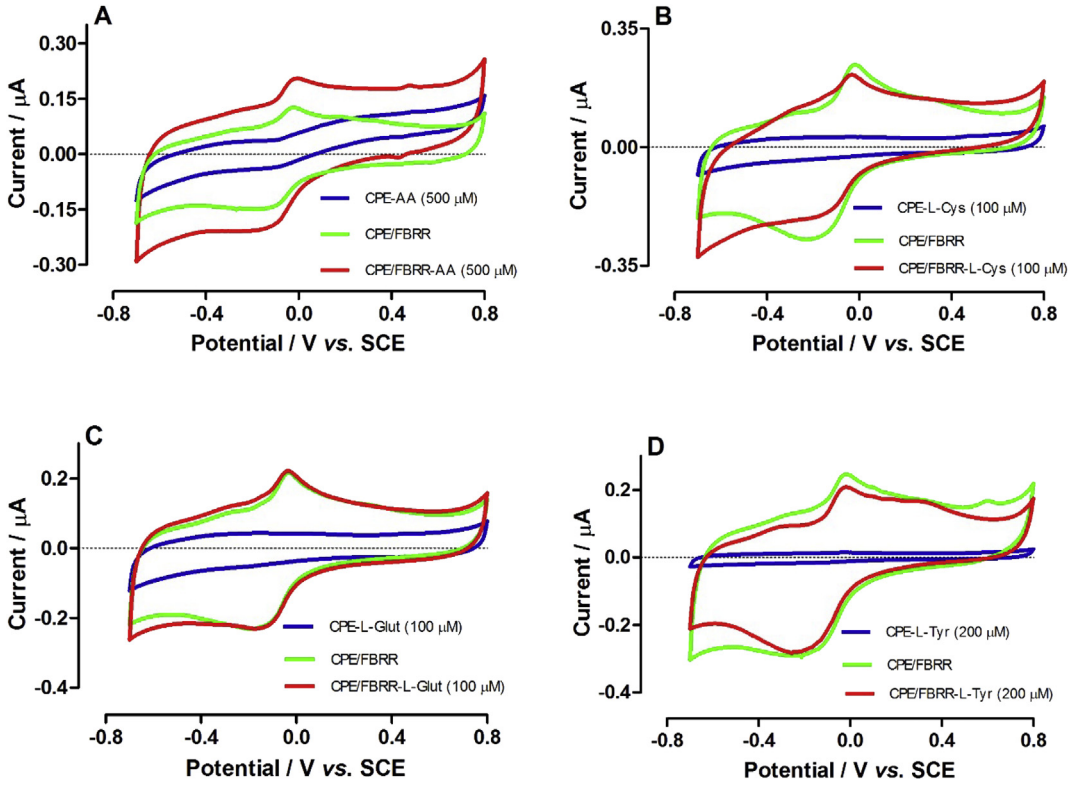

Fig. 3. Voltammograms recorded using FBBR-modified CPEs in the presence of physiological concentrations of electroactive interferents (A) 500 µM ascorbic acid (CPE/FBRR-AA) (B) 100 µM L-cysteine (CPE/FBRR-L-Cys) (C) 100 µM L-gluthathione (CPE/FBRR-L-Glut) and (D) 200 µM L-tyrosine (CPE/FBRR-L-Tyr). CPEs cycled over potential range − 0.7 V to +0.8 V *vs.* SCE at 100 mV/s ($n = 4$). Cycle 100 included for each CV.

3.5. Temperature effects

Heretofore, all previous experiments were carried out at room temperature, i.e. 22 °C. Since the principal objective of this work was to perform physiological monitoring, i.e. at 37 °C, it was critical to determine the effect of increasing temperature on the pH sensor's performance. The anodic peaks in Fig. 6A illustrate the corresponding potentials when cycling in PBS of varying pH. The first difference observed was the increased currents obtained with increased temperature due to an increase in the rate of the redox reaction. The second was the shift to a more negative potential for the values obtained at the higher temperature. This is because pH changes with temperature, according to the Rosenthal Correction Factor, by 0.015 pH units per °C [47]. This results in a shift of 0.225 pH units for the temperature difference of 15 °C. Assuming a Nernstian response of −59 mV/pH then the expected shift in peak potential is −13 mV. Therefore, if the peak potential at 22 °C is −34 mV, the expected peak potential at 37 °C would be −47 mV. Comparing the peak potentials at similar pH values between 22 °C and 37 °C in Fig. 6A gave potential shifts of approximately −20 mV (see Table SM2). Furthermore, the pH response is dependent on temperature according to:

$$\mathbf{m} = \mathbf{2.303}\boldsymbol{RT}/\boldsymbol{F} \quad (6)$$

Where m is the slope or pH response, R is the universal gas constant (J K^{-1} mol^{-1}), T represents the temperature (K) and F denotes the Faraday constant (C mol^{-1}). This results in a pH response of −62 mV/pH at a temperature of 37 °C. The pH responses at both temperatures are shown in Fig. 6A inset. They demonstrate excellent pH sensitivities with slopes of -59 ± 2 and -63 ± 1 mV/pH for 22 °C and 37 °C, respectively, with r^2 values > 0.99. This is in close agreement with the theoretical value of −62 mV/pH unit obtained from the Nernst equation for a 2 electron, 2 proton transfer at 37 °C. These sensitivities highlight the temperature dependence of the Nernst equation [48] and further demonstrate the efficacy of the developed sensor at measuring reliable pH shifts.

3.6. Ag/AgCl-PRE

To facilitate *in vivo* recordings, the SCE is normally replaced by a miniaturised PRE. It is extremely difficult to determine the precise potential of a PRE [49] which may compromise its utility in voltammetric measurements. Notwithstanding this, PREs have been extensively utilised for *in vivo* recordings in freely moving [33] and anaesthetised rodents [28]. Furthermore, it has been reported that PREs in PBS pH 7 maintain a constant potential [50], making them suitable for use in areas where the pH is regulated, e.g., biological systems. Therefore, it was vital to investigate the effect of changing reference electrodes on the quinone anodic peak potential. The anodic peaks from the resulting CVs are highlighted in Fig. 6B and clearly identify a shift in potential caused by using the Ag/AgCl-PRE, of approximately −34 mV, compared to the SCE. Literature values for the potential difference between Ag/AgCl and SCE reference electrodes suggest a shift of −44 mV [51]. There is also a clear shift in quinone peak potentials when changing the solution pH with linear regression analysis provided in Fig. 6B inset. There was no significant difference ($p = 0.47$) recorded between sensitivities recorded for the SCE (-57 ± 1 mV/pH, $n = 4$) and Ag/AgCl-PRE (-56 ± 1 mV/pH, $n = 4$). Despite obvious discrepancies in peak potentials between the two reference electrode systems, the extremely comparable sensitivities negate this issue. However, it is

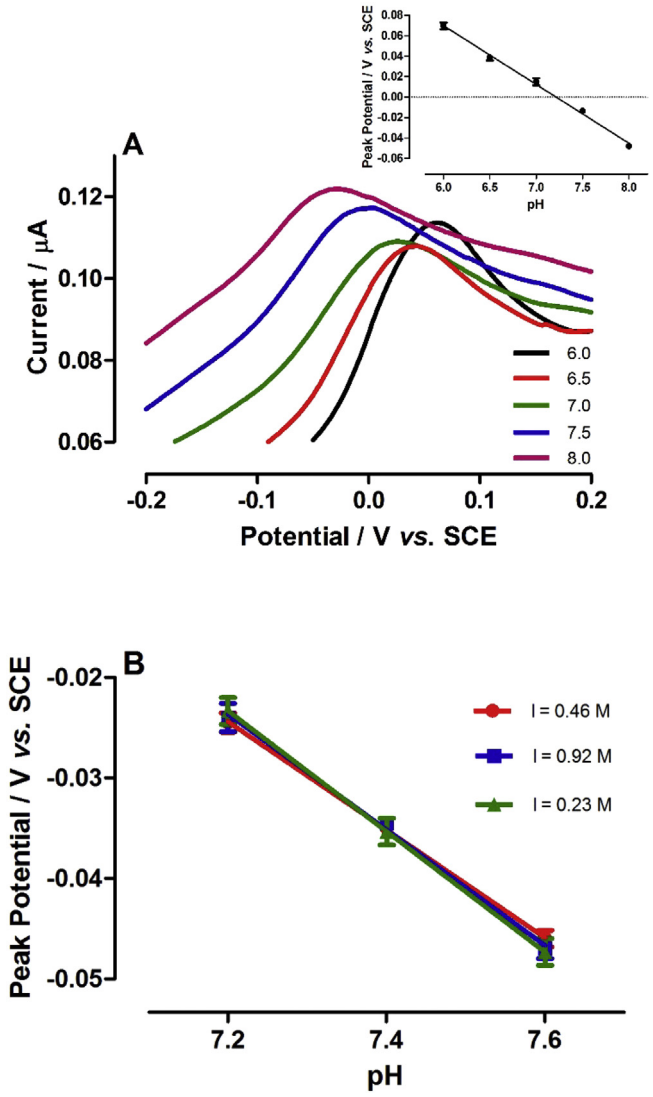

Fig. 4. (A) Comparison of pH sensitive quinone peaks of FBRR-modified CPEs ($n = 5$) cycled in PBS of pH 6.0 (black), pH 6.5 (red), pH 7.0 (green), pH 7.5 (blue) and pH 8.0 (purple). CPEs cycled over potential range −0.7 V to +0.8 V *vs.* SCE at 100 mV/s. Cycle 50 included for each pH. *Inset*: Corresponding potential-pH profile and linear regression analysis for oxidation peak potentials. (B) Potential-pH profiles and linear regression analysis comparing pH responses of FBRR-modified CPEs in solutions of varying ionic strength; 0.23 M (green), 0.46 M (red) and 0.92 M (blue). (For interpretation of the references to colour in this figure legend, the reader is referred to the Web version of this article.)

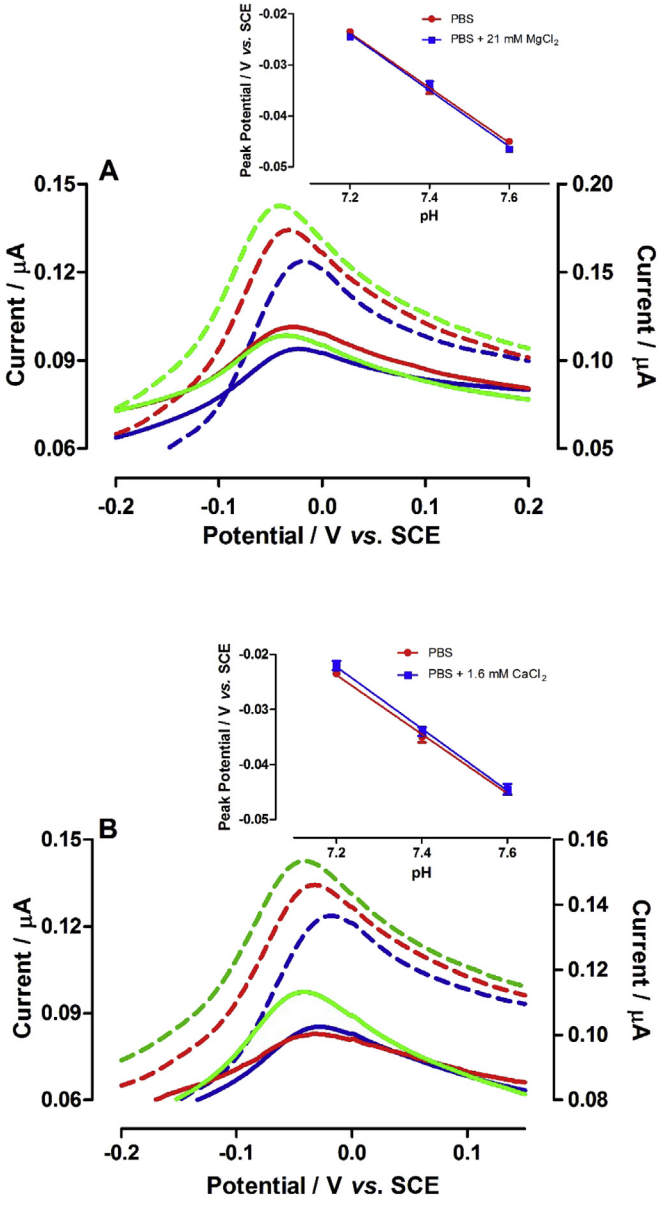

Fig. 5. Comparison of pH sensitive quinone peaks of FBRR-modified CPEs ($n = 4$) cycled in PBS of pH 7.2 (blue), 7.4 (red) and 7.6 (green) in the presence of (solid lines, right y-axes) and absence of (dashed lines, left y-axes) (A) 21 mM Mg^{2+} and (B) 1.6 mM Ca^{2+}. CPEs cycled over potential range −0.7 V to +0.8 V *vs.* SCE at 100 mV/s. Voltammograms performed at each 50th cycle included. *Insets:* corresponding potential-pH profiles and linear regression analysis ($n = 4$) performed in PBS with increase cation concentration (blue) and without (red). (For interpretation of the references to colour in this figure legend, the reader is referred to the Web version of this article.)

imperative that the difference in expected peak potentials is elucidated prior to deployment of this system in physiological media.

3.7. *In vivo* measurements in the hind limb of anaesthetised rats

Acute *in vivo* investigations were undertaken in the peripheral muscle of anaesthetised rats to confirm the efficacy of the FBRR-modified CPE at monitoring pH changes under physiological conditions. The CPEs were modified as described and implanted in combination with a Ag/AgCl-PRE and auxiliary electrode, through a hypodermic needle, into the hind limb of the anaesthetised subject. The CPE was cycled between −0.7 V and +0.8 V *vs.* Ag/AgCl at 100 mV/s. An initial baseline recording was performed over 90 cycles (45 min) to obtain a stable quinone peak potential and this is detailed in Fig. SM4B. Using the dashed line as a point of reference, it is clear that the stability of the peak is retained over the 90 cycles. Moreover, the 90th cycle, recorded at the end of the settling phase, had its peak potential located at *ca.* −82 mV *vs.* Ag/AgCl which equates to a pH of 7.60 using the potential responses described for Ag/AgCl-PRE in the previous section and detailed in Table SM2. However, it is important to emphasise that these potentials were obtained at 22 °C and it is imperative that we incorporate the effect of increased temperature when determining the baseline pH levels, i.e. −20 mV shift between 22 °C and 37 °C. This postulates a potential of −62 mV at 22 °C which is closer to a baseline pH level of 7.25. This is in close alignment to *in vivo* baseline levels recorded

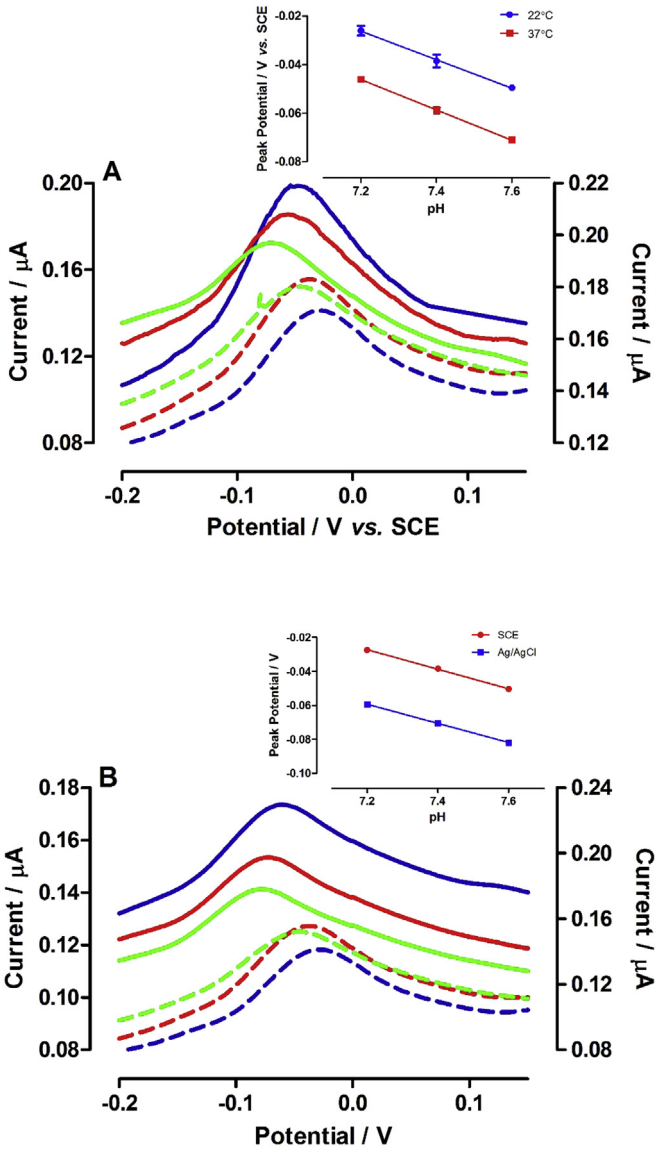

Fig. 6. Comparison of pH sensitive quinone peaks of FBRR-modified CPEs cycled in PBS of pH 7.2 (blue), 7.4 (red) and 7.6 (green) recorded (A) at 22 °C (dashed line, left y-axis) and 37 °C (solid line, right y-axis) and (B) using a Ag/AgCl-pseudo reference electrode (PRE) (solid lines, right y-axis) and a SCE (dashed lines, left y-axis). CPEs cycled over potential range −0.7 V to +0.8 V *vs.* SCE at 100 mV/s. Voltammograms performed at each 50th cycle included. *Insets:* corresponding potential-pH profiles and linear regression analysis ($n = 4$) performed at 22 °C (blue)/37 °C (red) and using Ag/AgCl PRE (blue)/SCE (red). (For interpretation of the references to colour in this figure legend, the reader is referred to the Web version of this article.)

previously in the brains of rodents which is extremely encouraging [18,19,33].

Two perturbations were performed in separate animal cohorts to determine the efficacy of the FBRR-modified CPE at monitoring shifts in muscle pH. Localised changes in pH were brought about by the induction of ischaemia to reduce the pH or by the injection of bicarbonate ions to increase pH. After a short recording time period, the tissue pH was allowed to recover. Reduced blood flow results in tissue ischaemia, causing insufficient oxygen and nutritional requirements, starving the affected tissue of its metabolic needs. The reduced oxygen supply to the tissue causes cell metabolism to change from aerobic to anaerobic which results in the production of lactic acid. This, along with increased levels of CO_2, induces a decrease in pH levels [52]. A tourniquet was applied to the hind limb to induce ischaemia using a model previously described [28]. Fig. 7A and SM4A illustrate the quinone peak potential shift over the duration of the 200 cycles (100 min). The inset in Fig. 7A highlights the shaded area and red arrows indicate the application of ischaemic insult. There was an obvious increase in quinone peak potential observed, from a pre-insult level of −52 mV, to a maximum response of −17 mV *vs.* Ag/AgCl, over the course of the tourniquet application. This group of FBRR-modified CPEs had an *in vitro* pH sensitivity of −57 ± 2 mV/pH ($n = 4$), corresponding to a shift of 0.65 pH units resulting from the ischemic episode. This decrease is consistent with literature values reporting a pH drop of 0.70 pH units after 60 min [53]. During ischaemia, tissue pH can drop to as low as 6.0–6.5 *in-vivo* [54]. It is detailed in Fig. 4A that linearity is retained at these lower pH values, supporting the accuracy of our sensor data. Post-ischemic insult, the tissue was shown to rapidly return and slightly overshoot the pre-insult baseline, a potential shift from −17 mV to −55 mV *vs.* Ag/AgCl, indicating tissue reperfusion. This corroborates findings using a tissue oxygen sensor in the same animal model, whereby a rapid

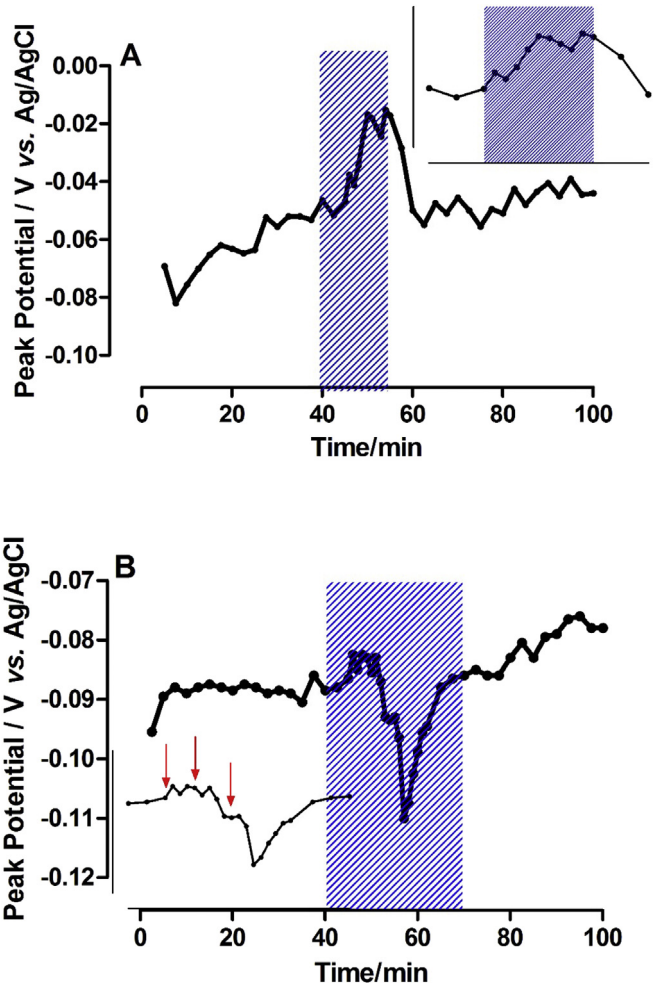

Fig. 7. *In vivo* recordings performed using FBRR-modified CPEs in the hind-limb of anaesthetised wistar rats over the potential range − 0.7 V to +0.8 V *vs.* Ag/AgCl at 100 mV/s. Average potential-time profiles from FBRR-modified CPEs in (A) hind-limb model of ischaemia to lower tissue pH ($n = 4$) and (B) injection of sodium bicarbonate to increase tissue pH ($n = 4$). *Insets*: close-up of shaded areas representative of perturbation. Red arrows indicate start/end of ischaemic insult (A) and various injections of sodium bicarbonate (B). (For interpretation of the references to colour in this figure legend, the reader is referred to the Web version of this article.)

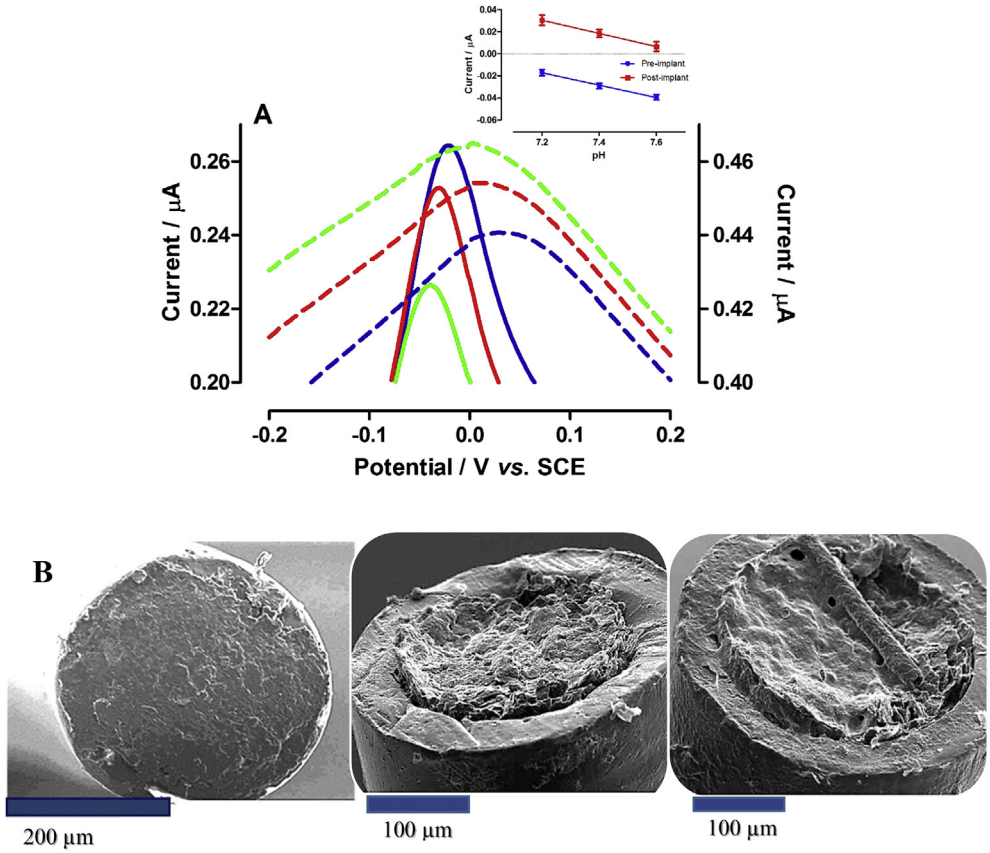

Fig. 8. (A) Comparison of pH sensitive quinone peaks of FBRR-modified CPEs ($n = 4$) cycled in PBS of pH 7.2 (blue), 7.4 (red) and 7.6 (green) recorded pre-implantation (solid line, right y-axis) and post implantation (dashed lines, left y-axis) *in vivo*. CPEs cycled over potential range −0.7 V to +0.8 V *vs.* SCE at 100 mV/s. Voltammograms performed at each 50th cycle included. *Inset*: corresponding potential-pH profiles and linear regression analysis ($n = 4$) for pre-implanted (blue trace) and post implanted (red trace) FBRR-modified CPEs. (B) SEM images illustrating pre-implanted (left) and post-implanted (centre, right) FMRR-modified CPEs. (For interpretation of the references to colour in this figure legend, the reader is referred to the Web version of this article.)

overshoot in oxygen levels follows the 10-min insult [28]. The increase in pH can be explained by reperfusion following restoration of vasculature supply and aerobic metabolism. This finding strongly supports the efficacy of the FBRR-modified CPE at measuring a decrease in physiological pH.

To induce an increase in pH levels, injections of sodium bicarbonate [30–32], a weak base, were administered locally to the hind limb of the animals. Bicarbonate therapy is a known treatment administered to patients suffering from the effects of acidosis [32]. Fig. 7B and SM4C highlight the quinone peak potential shift over the duration of the 200 cycles (100 min). The inset highlights the shaded area and red arrows indicate the injections of 45 mM sodium bicarbonate. It was apparent that, immediately after the 1st and 2nd injections, there was an unexpected increase in the peak potential, which was interpreted as injection stress. However, a large drop in quinone peak potential was recorded over the course of the 2nd and 3rd injections with a maximum potential of −110 mV recorded. This maximum drop in peak potential corresponded to a pH rise of 0.61 pH units ($n = 4$), indicating severe alkalemia [55] or alkalosis. The peak potential returned to a pre-injection level of −88 mV after 65 min (20-min post-injection) illustrating the ability of the physiological tissue to correct the pH shift in a timely manner. Once again, these findings strongly support the efficacy of the FBRR-modified CPE at measuring a deviation in physiological pH and demonstrates its *in vivo* utility.

Finally, post *in vivo* calibrations were performed on the implanted FBRR-modified CPEs. The average sensitivity recorded was -60 ± 1 mV/pH ($n = 4$, $r^2 > 0.99$) which was not significantly different than the pre-implantation sensitivity (-57 ± 2 mV/pH, $n = 4$, $r^2 > 0.99$). However, it is obvious from Fig. 8A that the resolution of the quinone peak has been compromised with a concomitant shift in the peak potential observed. This supports our sensocompatability findings; in particular Fig. SM1, where a broadening of the quinone peak, after 24 h storage in proteins and lipids was recorded, along with a shift in the peak potential also. The SEM images in Fig. 8B illustrate discrepancies in the surface morphology of the pre-implanted and post-implanted CPEs which is not entirely unexpected. The smooth surface of the CPE in the left image is replaced by an uneven, concave shaped surface in the centre and right sided image. The altered surface is more than likely caused by a combination of proteins and lipids coupled with physical damage caused by the removal process which could give rise to the broader peaks observed in Fig. 8A. Notwithstanding this, improved peak resolution was observed for sensocompatability studies performed during continuous cycling in proteins and lipids and more importantly during *in vivo* recordings (see Fig. SM4B). Collectively, these findings support the functionality of the FBRR-modified CPE during *in vivo* recordings and demonstrate retention of the electrodeposited diazonium salt on the CPE surface following exposure to physiological conditions.

4. Conclusion

We have presented the *in vitro* characterisation and *in vivo* validation of a FBRR-modified CPE for the physiological monitoring of pH. An in-depth characterisation supported the ability of the

modified electrode to perform stable measurements during continuous cycling in solutions of protein and lipid, for a minimum of 9 h. Furthermore, peak resolution and stability were retained in the presence of an abundance of physiological interferents identified from both peripheral and brain extracellular fluid. There was no effect on sensor performance due to variations in ionic strength and cation concentrations. In addition, the influence of temperature and reference electrodes were elucidated to facilitate accurate pH monitoring under physiological conditions. Finally, the FBRR-modified CPE demonstrated the ability to monitor pH changes in the muscle tissue of anaesthetised rats exposed to ischaemia and injections of sodium bicarbonate. Post-implantation calibrations demonstrated no significant difference in sensitivity when compared against pre-implanted values. The work described strongly supports the ability of the FBRR-modified CPE to measure accurate changes in peripheral tissue pH. Furthermore, the work supports its deployment in brain applications also.

Conflict of interest

The authors have no conflict of interest.

Acknowledgements

All work described within was undertaken through financial support from the Irish Research Council (Grant no. RS/2012/79). We also extend our gratitude to Prof. John Lowry for providing access to infrastructure.

Appendix A. Supplementary data

Supplementary data to this article can be found online at https://doi.org/10.1016/j.electacta.2018.12.110.

References

[1] N. McVicar, A.X. Li, D.F. Gonçalves, M. Bellyou, S.O. Meakin, M.A.M. Prado, R. Bartha, Quantitative tissue pH measurement during cerebral ischemia using amine and amide concentration-independent detection (AACID) with MRI, J. Cerebr. Blood Flow Metabol. 34 (2014) 690–698.
[2] M.A. Makos, D.M. Omiatek, A.G. Ewing, M.L. Heien, Development and characterization of a voltammetric carbon-fiber microelectrode pH sensor, Langmuir 26 (2010) 10386–10391.
[3] H. Hayakawa, D.J. Aldington, M. A.M., Acute traumatic compartment syndrome: a systematic review of results of fasciotomy, Trauma 11 (2009) 5–35.
[4] A. Tiwari, A.I. Haq, F. Myint, G. Hamilton, Acute compartment syndromes, Br. J. Surg. 89 (2002) 397–412.
[5] M. Teraa, M.S. Conte, F.L. Moll, M.C. Verhaar, Critical limb ischemia: current trends and future directions, J. Am. Heart Assoc. 5 (2016) e002938–e002946.
[6] D.K. Harrison, W.F. Walker, Tissue pH electrodes for clinical applications, J. Med. Eng. Technol. 4 (1980) 3–7.
[7] P.W. Wolpert, D. Shaughnessy, D.N. Houchin, M.E. Baccari, F.A. Miller, Tissue pH: a new clinical tool, Arch. Surg. 101 (1970) 308–313.
[8] D. Ellis, R.C. Thomas, Direct measurement of the intracellular pH of mammalian cardiac muscle, J. Physiol. 262 (1976) 755–771.
[9] D.K. Harrison, W.F. Walker, Micro-electrode measurement of skin pH in humans during ischaemia, hypoxia and local hypothermia, J. Physiol. 291 (1979) 339–350.
[10] M.J. Martin, P. Rolfe, Potentiometric methods of in vivo analysis, Anal. Processes 23 (1986) 303–304.
[11] X.-r. Huang, Q.-q. Ren, X.-j. Yuan, W. Wen, W. Chen, D.-P. Zhan, Iridium oxide based coaxial pH ultramicroelectrode, Electrochem. Commun. 40 (2014) 35–37.
[12] A. Eftekhari, pH sensor based on deposited film of lead oxide on aluminum substrate electrode, Sensor. Actuator. B 88 (2003) 234–238.
[13] T.-F. Kang, Z.-Y. Xie, H. Tang, G.-L. Shen, R.-Q. Yu, Potentiometric pH sensors based on chemically modified electrodes with electropolymerized metal-tetraaminophthalocyanine, Talanta 45 (1997) 291–296.
[14] D. O'Hare, K.H. Parker, C.P. Winlove, Metal-metal oxide pH sensors for physiological application, Med. Eng. Phys. 28 (2006) 982–988.
[15] M. Lu, R.G. Compton, Voltammetric pH sensor based on an edge plane pyrolytic graphite electrode, Analyst 139 (2014) 2397–2403.
[16] M. Lu, R.G. Compton, Voltammetric pH sensing using carbon electrodes: glassy carbon behaves similarly to EPPG, Analyst 139 (2014) 4599–4605.
[17] M. Michalak, M. Kurel, J. Jedraszko, D. Toczydlowska, G. Wittstock, M. Opallo, W. Nogala, Voltammetric pH nanosensor, Anal. Chem. 87 (2015) 11641–11645.
[18] F. Zhao, L.M. Zhang, A.W. Zhu, G.Y. Shi, Y. Tian, In vivo monitoring of local pH values in a live rat brain based on the design of a specific electroactive molecule for H+, Chem. Commun. 52 (2016) 3717–3720.
[19] J. Zhou, L.M. Zhang, Y. Tian, Micro electrochemical pH sensor applicable for real-time ratiometric monitoring of pH values in rat brains, Anal. Chem. 88 (2016) 2113–2118.
[20] O. Korostynska, K. Arshak, E. Gill, A. Arshak, Review paper: materials and techniques for in vivo pH monitoring, IEEE Sensor. J. 8 (2008) 20–28.
[21] R.B. Easley, T.R. Johnson, J.D. Tobias, Continuous pH monitoring using the Paratrend 7 inserted into a peripheral vein in a patient with shock and congenital lactic acidosis, Clin. Pediatr. 41 (2002) 351–355.
[22] B.R. Soller, Y. Yang, S.M.C. Lee, C. Wilson, R.D. Hagan, Non-invasive determination of exercise-induced hydrogen ion threshold through direct optical measurement, J. Appl. Physiol. 104 (2008) 837–844.
[23] P. Lipton, Ischemic cell death in brain neurons, Physiol. Rev. 79 (1999) 1431–1568.
[24] R.D. O'Neill, Long-term monitoring of brain dopamine metabolism in vivo with carbon paste electrodes, Sensors 5 (2005) 317–342.
[25] P.D. Lyne, R.D. O'Neill, Stearate-modified carbon paste electrodes for detecting dopamine in vivo: decrease in selectivity caused by lipids and other surface-active agents, Anal. Chem. 62 (1990) 2347–2351.
[26] K.M. Herdman, C.B. Breslin, N.J. Finnerty, The aqueous deposition of a pH sensitive quinone on carbon paste electrodes using linear sweep voltammetry, J. Electroanal. Chem. 828 (2018) 137–143.
[27] C.H. Reid, N.J. Finnerty, Long term amperometric recordings in the brain extracellular fluid of freely moving immunocompromised NOD SCID mice, Sensors 17 (2017) 419–434.
[28] N.J. Finnerty, F.B. Bolger, In vitro development and in vivo application of a platinum-based electrochemical device for continuous measurements of peripheral tissue oxygen, Bioelectrochemistry 119 (2018) 124–135.
[29] E. Gnaiger, G. Mendez, S.C. Hand, High phosphorylation efficiency and depression of uncoupled respiration in mitochondria under hypoxia, Proc. Natl. Acad. Sci. 97 (2000) 11080–11085.
[30] D.W. Richardson, A.J. Wasserman, J.L. Patterson Jr., General and regional circulatory responses to change in blood pH and carbon dioxide tension, J. Clin. Invest. 40 (1961) 31–43.
[31] S.A. Grant, K. Bettencourt, P. Krulevitch, J. Hamilton, R. Glass, In vitro and in vivo measurements of fiber optic and electrochemical sensors to monitor brain tissue pH, Sensor. Actuator. B 72 (2001) 174–179.
[32] E.M. Ostrea Jr., G.B. Odell, Influence of bicarbonate administration on blood pH in a closed system. Clinical implications, J. Pediatr. 80 (1972) 671–680.
[33] N.J. Finnerty, F.B. Bolger, A platinum oxide-based microvoltammetric pH electrode suitable for physiological investigations, Analyst 143 (2018) 3124–3133.
[34] F.O. Brown, N.J. Finnerty, J.P. Lowry, Nitric oxide monitoring in brain extracellular fluid: characterisation of Nafion (R)-modified Pt electrodes in vitro and in vivo, Analyst 134 (2009) 2012–2020.
[35] A.M. Wynne, C.H. Reid, N.J. Finnerty, In vitro characterisation of ortho phenylenediamine and Nafion-modified Pt electrodes for measuring brain nitric oxide, J. Electroanal. Chem. 732 (2014) 110–116.
[36] D.A. Kane, R.D. O'Neill, Major differences in the behaviour of carbon paste and carbon fibre electrodes in a protein-lipid matrix: implications for voltammetry in vivo, Analyst 123 (1998) 2899–2903.
[37] D.E. Ormonde, R.D. O'Neill, The oxidation of ascorbic acid at carbon paste electrodes. Modified response following contact with surfactant, lipid and brain tissue, J. Electroanal. Chem. Interfacial Electrochem. 279 (1990) 109–121.
[38] D. Shin, D.A. Tryk, A. Fujishima, A. Merkoci, J. Wang, Resistance to surfactant and protein fouling effects at conducting diamond electrodes, Electroanalysis 17 (2005) 305–311.
[39] S.S. Shankar, B.E.K. Swamy, B.N. Chandrashekar, Electrochemical selective determination of dopamine at TX-100 modified carbon paste electrode: a voltammetric study, J. Mol. Liq. 168 (2012) 80–86.
[40] B.M. Weidgans, C. Krause, I. Klimant, O.S. Wolfbeis, Fluorescent pH sensors with negligible sensitivity to ionic strength, Analyst 129 (2004) 645–650.
[41] D. Veloso, R.W. Guynn, M. Oskarsson, R.L. Veech, Concentrations of free and bound magnesium in rat tissues. Relative constancy of free magnesium ion concentrations, J. Biol. Chem. 248 (1973) 4811–4819.
[42] M. Walser, Magnesium metabolism, Ergebnisse der Physiologie 59 (1967) 185–296.
[43] M.M. Dvorak, A. Siddiqua, D.T. Ward, D.H. Carter, S.L. Dallas, E.F. Nemeth, D. Riccardi, Physiological changes in extracellular calcium concentration directly control osteoblast function in the absence of calciotropic hormones, Proc. Natl. Acad. Sci. U. S. A 101 (2004) 5140–5145.
[44] G.G. Wildgoose, M. Pandurangappa, N.S. Lawrence, L. Jiang, T.G.J. Jones, R.G. Compton, Anthraquinone-derivatised carbon powder: reagentless voltammetric pH electrodes, Talanta 60 (2003) 887–893.
[45] M.C. Mahedero, M. Roman Ceba, A. Fernandez-Gutierrez, 1,8-Dihydroxyanthraquinone-calcium(II) reaction. Spectrofluorometric determination of traces of calcium(II), Anal. Lett. 19 (1986) 1725–1730.
[46] P.S. Guin, S. Das, P.C. Mandal, Electrochemical reduction of quinones in different media: a review, Int. J. Electrochem. Sc. 2011 (2011)

816202–816222.
[47] E.R. Ashwood, G. Kost, M. Kenny, Temperature correction of blood-gas and pH measurements, Clin. Chem. 29 (1983) 1877–1885.
[48] H.C. Leventis, I. Streeter, G.G. Wildgoose, N.S. Lawrence, L. Jiang, T.G.J. Jones, R.G. Compton, Derivatized carbon powder electrodes: reagentless pH sensors, Talanta 63 (2004) 1039–1051.
[49] M.W. Shinwari, D. Zhitomirsky, I.A. Deen, P.R. Selvaganapathy, M.J. Deen, D. Landheer, Microfabricated reference electrodes and their biosensing applications, Sensors 10 (2010) 1679–1715.
[50] T. Matsumoto, A. Ohashi, N. Ito, Development of a micro-planar Ag/AgCl quasi-reference electrode with long-term stability for an amperometric glucose sensor, Anal. Chim. Acta 462 (2002) 253–259.
[51] D. Desmond, B. Lane, J. Alderman, J.D. Glennon, D. Diamond, D.W.M. Arrigan, Evaluation of miniaturized solid state reference electrodes on a silicon based component, Sensor. Actuator. B 44 (1997) 389–396.
[52] S. Kun, B. Ristic, R.A. Peura, R.M. Dunn, Algorithm for tissue ischemia estimation based on electrical impedance spectroscopy, IEEE Trans. Biomed. Eng. 50 (2003) 1352–1359.
[53] D. Troitzsch, S. Vogt, H. Abdul-Khaliq, R. Moosdorf, Muscle tissue oxygen tension and oxidative metabolism during ischemia and reperfusion, J. Surg. Res. 128 (2005) 9–14.
[54] A.-D. Andersen, K.A. Poulsen, I.H. Lambert, S.F. Pedersen, HL-1 mouse cardiomyocyte injury and death after simulated ischemia and reperfusion: roles of pH, Ca2+-independent phospholipase A2, and Na+/H+ exchange, Am. J. Physiol. 296 (2009) C1227–C1242.
[55] H.J. Adrogue, N.E. Madias, Management of life-threatening acid-base disorders. Second of two parts, N. Engl. J. Med. 338 (1998) 107–111.